Role of the Soffer bound in determination of transversity and the tensor charge

Umberto D'Alesio[a,b], Carlo Flore[a,b,c,*], Alexei Prokudin[d,e]

[a] *Dipartimento di Fisica, Università di Cagliari, Cittadella Universitaria, I-09042 Monserrato (CA), Italy*
[b] *INFN, Sezione di Cagliari, Cittadella Universitaria, I-09042 Monserrato (CA), Italy*
[c] *Laboratoire de Physique des 2 Infinis Irène Joliot-Curie, CNRS, Université Paris-Saclay, 91406 Orsay Cedex, France*
[d] *Division of Science, Penn State University Berks, Reading, Pennsylvania 19610, USA*
[e] *Theory Center, Jefferson Lab, 12000 Jefferson Avenue, Newport News, Virginia 23606, USA*

Abstract

The transversity and the tensor charge of the nucleon, currently under active investigation experimentally and theoretically, are fundamental quantities in hadron physics and for our comprehension of the nucleon structure. Some tension between the values of the tensor charge, as computed on the basis of phenomenological extractions and lattice QCD calculations, has been observed. In this letter, by means of an explicit example, we study the role of assumptions, usually adopted in phenomenological parametrizations, and we show that, by relaxing some of them, such a tension could be eased.

Keywords: transversity function, Soffer bound, tensor charge, QCD

1. Introduction

The collinear transversity function [1], $h_1^q(x)$, together with the unpolarized $f_{q/p}(x)$ and the helicity g_{1L}^q parton distribution functions, describe the collinear structure of a spin-1/2 hadron at leading twist. Unlike $f_{q/p}(x)$ and g_{1L}^q, $h_1^q(x)$, being a chiral-odd quantity, cannot be directly accessed in inclusive deep-inelastic scattering process (DIS), as another chiral-odd function is needed to form a chiral even observable. At present, transversity has been extracted [2–5] in Semi Inclusive Deep Inelastic Scattering (SIDIS) processes in combination with the Collins fragmentation function (FF) [6], or in two-hadron production in combination with a polarized dihadron fragmentation function [7–11].

The possibility of accessing transversity in double polarized Drell-Yan process and a careful study of its properties and related sum rules were explored by Jaffe and Ji in Ref. [12]. The Q^2 evolution of transversity was investigated by Artru and Mekhi in Ref. [13] in leading order (LO) QCD. Soffer derived a positivity bound for transversity [14], referred to as Soffer bound (SB). In Ref. [15] Barone showed that the SB, if true at some initial scale Q_0, is preserved by QCD evolution at LO. Vogelsang, in Ref. [16], extended this result showing that SB is preserved at next-to-leading order (NLO) accuracy as well.

The validity of the bound itself was questioned by Ralston in Ref. [17]. On the other hand, it is a suitable tool and different research groups have used the SB in their phenomenological extractions [4, 10, 11, 18]. The x-dependent part of h_1^q is usually parametrized in terms of such bound at Q_0, the initial scale of the analysis. By imposing suitable constraints on the fit parameters, the Soffer bound is automatically fulfilled throughout the analysis. At variance, the recent study of Ref. [11] adopts the method of Lagrange multipliers to constrain transversity with a flexible parametrization of h_1^q.

Studies of transversity and the tensor charge are important for Beyond Standard Model searches. Indeed, the isovector tensor charge, g_T, is related to potential tensor interactions in the electroweak sector [19–22], and it is usually calculated on the lattice, as a matrix element over the full x range, or by integrating the extracted transversity functions from phenomenological analyses. With respect to lattice QCD estimates, the latest phenomenological extractions of the transversity function [3, 5, 9, 10, 18, 23, 24] seem to show a tension [25] on the estimated values of g_T as well as on individual contributions from up, δu, and down, δd, quarks (see Eq. (15) below).

To this extent, it is interesting to check what is the role of the underlying assumptions adopted in phenomenological analyses. In this letter, by using an explicit example, we explore the impact of loosening some of these choices. This would bring us to analyze several aspects, such as the parameter-space exploration, whether we observe the violation of the Soffer bound in existing data and how all of this traduces into (isovector) tensor charge estimates.

The rest of the letter is organized as follows: in Section 2 we present the results of global fits of the transversity function from SIDIS and e^+e^- data, obtained in the framework of the transverse momentum dependent (TMD) approach. Then, in Section 3, we will investigate the im-

*Corresponding author
Email addresses: umberto.dalesio@ca.infn.it (Umberto D'Alesio), flore@ipno.in2p3.fr (Carlo Flore), prokudin@jlab.org (Alexei Prokudin)

pact of these results in estimating the tensor charges. Conclusions and comments are finally gathered in Section 4.

2. Transversity from SIDIS data and role of the Soffer bound

The bound [14], derived by Soffer, reads:

$$|h_1^q(x,Q^2)| \leq \frac{1}{2}\left[f_{q/p}(x,Q^2) + g_{1L}^q(x,Q^2)\right] \equiv \mathrm{SB}(x,Q^2), \tag{1}$$

where $f_{q/p}(x)$ and $g_{1L}^q(x)$ are respectively the unpolarized and the helicity parton distribution functions (PDFs).

Transversity has been extracted [26–29] in SIDIS, by analysing the so-called Collins asymmetry:

$$A_{UT}^{\sin(\phi_h+\phi_S)} = \frac{2(1-y)}{1+(1-y)^2}\frac{F_{UT}^{\sin(\phi_h+\phi_S)}}{F_{UU}}\,, \tag{2}$$

where y is the fractional energy loss of the incident lepton, $F_{UU} = \mathcal{C}[f_1 D_1]$ is the unpolarized structure function and $F_{UT}^{\sin(\phi_h+\phi_S)} = \mathcal{C}[h_1 H_1^\perp]$ [30–32] is the polarized structure function of the SIDIS cross section, given as a convolution (over the unobserved transverse momenta) of the transversity TMD distribution, h_1^q, and the Collins FF, $H_1^\perp$.

In order to unravel the transversity, one has to gather additional information on the Collins FFs, that could be accessed in $e^+e^- \to h_1 h_2 X$ processes via a $\cos(2\phi_0)$ modulation, $A_0^{UL(C)} \propto \mathcal{C}[\bar{H}_1^\perp H_1^\perp]$ [33]. This was measured at the energy $\sqrt{s} \simeq 10.6$ GeV by the BELLE [34] and the BABAR [35] Collaborations as well as by the BESIII [36] Collaboration, at a lower energy, $\sqrt{s} \simeq 3.65$ GeV.

Collins asymmetries in SIDIS and e^+e^- processes at low values of transverse momentum (of the final hadron or of the almost back-to-back hadron pair) are formally expressed in terms of a TMD factorization approach [32, 33]. The TMD transversity function $h_1^q(x,k_\perp)$, related to its collinear counterpart $h_1^q(x)$, was extracted in a series of global TMD fits of SIDIS and $e^+e^- \to h_1 h_2 X$ data [3, 18, 23].

Complementary information on the collinear transversity function is obtained also in the context of a collinear framework, for instance by considering its convolution with di-hadron FFs in pion-pair production in SIDIS [9, 11, 24] and in polarized pp collisions [10].

2.1. Fitting the TMD transversity function

In this Section we present the results of our fits performed within a TMD approach. We will discuss and quantify the influence of initial assumptions and their impact on the extracted transversity functions.

Our analysis has been carried out following the model of Ref. [18], to which we refer the reader for all explicit expressions of the observables within the adopted parametrization. Here we will highlight the differences with respect to the analysis of Ref. [18] starting from the new dataset: in addition to the SIDIS $A_{UT}^{\sin(\phi_h+\phi_S)}$ data from HERMES off a proton target [37] and COMPASS off proton [28] and deuteron [27] targets, and e^+e^- $A_0^{UL(C)}$ data from Belle [34] and Babar [35], we have also included the latest BESIII data [36] for e^+e^- azimuthal correlations. This results in a total number of datapoints $N_{\rm pts} = 278$.

In the analysis of Ref. [18] and Refs. [3, 23], transversity was parametrized adopting the usual Gaussian ansatz, with factorized x and $k_\perp$ dependences, as

$$h_1^q(x,k_\perp^2) = h_1^q(x)\frac{e^{-k_\perp^2/\langle k_\perp^2\rangle}}{\pi\langle k_\perp^2\rangle}. \tag{3}$$

We will use $\langle k_\perp^2\rangle = 0.57$ (GeV^2), as extracted from HERMES multiplicities in Ref. [38]. The x-dependent part of transversity is usually parametrized [3, 18, 23] at the initial scale Q_0^2 in terms of the Soffer bound, as

$$h_1^q(x,Q_0^2) = \mathcal{N}_q^T(x)\,\mathrm{SB}(x,Q_0^2). \tag{4}$$

For the Soffer bound, Eq. (1), we adopt one of the most recent extractions of the collinear helicity distributions, namely the NLO DSSV set of Ref. [39]. For consistency, for the collinear unpolarized PDFs and FFs we adopt the NLO CTEQ66 PDFs set [40] and the NLO DSS 2014 pion FFs set [41]. A transversity DGLAP kernel is then employed to carry out the evolution up to higher values of Q^2, by using an appropriately modified version [42, 43] of `HOPPET` code [44]. We adopt $Q_0^2 = 1.69\,\mathrm{GeV}^2$ as the input scale, with $\alpha_S(M_Z) \simeq 0.118$ according to the CTEQ66 scheme. The $\mathcal{N}_q^T(x)$ factor in Eq. (4) is given by

$$\mathcal{N}_q^T(x) = N_q^T x^\alpha (1-x)^\beta \frac{(\alpha+\beta)^{\alpha+\beta}}{\alpha^\alpha\beta^\beta}, \quad (q = u_v,\, d_v) \tag{5}$$

with the same α and β parameters for the valence u_v and d_v transversity functions.

Upon constraining

$$|N_q^T| \leq 1\,, \tag{6}$$

the transversity functions automatically fulfill their corresponding Soffer bound in Eq. (1). Such constraint plays an important role in the extraction of the transversity function. To study and quantify the influence of the choice in Eq. (6) we will perform two fits of the data using (and not using) such a condition on N_q^T parameters, i.e. ensuring (not ensuring) the automatic fulfilment of the SB throughout the fit. In the plots shown below, we will respectively refer to these two cases as "using SB" or "no SB".

The Collins functions are parametrized as in Ref. [18]

$$H_1^{\perp q}(z,p_\perp^2) = \mathcal{N}_q^C(z)\frac{z m_h}{M_C}\sqrt{2e}\,e^{-p_\perp^2/M_C^2}\,D_{h/q}(z,p_\perp^2)\,, \tag{7}$$

with $q = \mathrm{fav}, \mathrm{unf}$ (favoured/unfavoured) and where M_C is a free parameter with mass dimension. $D_{h/q}(z,p_\perp^2)$ is the unpolarized TMD fragmentation function

$$D_{h/q}(z,p_\perp^2) = D_{h/q}(z)\,\frac{e^{-p_\perp^2/\langle p_\perp^2\rangle}}{\pi\langle p_\perp^2\rangle}\,, \tag{8}$$

with $\langle p_\perp^2 \rangle = 0.12$ GeV^2 [38]; for $D_{h/q}(z)$ we use the NLO DSS 2014 set [41]. The $\mathcal{N}_q^C(z)$ factors are given by

$$\mathcal{N}_{\rm fav}^C(z) = N_{\rm fav}^C\, z^\gamma (1-z)^\delta \frac{(\gamma+\delta)^{\gamma+\delta}}{\gamma^\gamma \delta^\delta}\,, \qquad \mathcal{N}_{\rm unf}^C(z) = N_{\rm unf}^C\,. \tag{9}$$

In order to estimate the errors of the extracted functions, we will follow the procedure of Ref. [45], and for a given observable $\mathcal{O}$ we compute the expectation value $\mathrm{E}[\mathcal{O}]$ and variance $\mathrm{V}[\mathcal{O}]$ as

$$\mathrm{E}[\mathcal{O}] = \int d^n a\, \mathcal{P}(\boldsymbol{a}|\mathrm{data})\, \mathcal{O}(\boldsymbol{a}) \simeq \sum_k w_k\, \mathcal{O}(\boldsymbol{a}_k)\,, \tag{10}$$

$$\mathrm{V}[\mathcal{O}] = \int d^n a\, \mathcal{P}(\boldsymbol{a}|\mathrm{data})\, (\mathcal{O}(\boldsymbol{a}) - \mathrm{E}[\mathcal{O}])^2 \simeq \sum_k w_k\, (\mathcal{O}(\boldsymbol{a}_k) - \mathrm{E}[\mathcal{O}])^2\,. \tag{11}$$

$\mathcal{O}$ is a function of the n-dimensional parameter vector $\boldsymbol{a}$ with a multivariate probability density $\mathcal{P}(\boldsymbol{a}|\mathrm{data})$ [45] for parameters $\boldsymbol{a}$ conditioned by existing experimental data. This can be written using Bayes' theorem as

$$\mathcal{P}(\boldsymbol{a}|\mathrm{data}) = \frac{\mathcal{L}(\mathrm{data}|\boldsymbol{a})\,\pi(\boldsymbol{a})}{\mathrm{Z}}\,, \tag{12}$$

where $\mathcal{L}(\mathrm{data}|\boldsymbol{a})$ is the likelihood, $\pi(\boldsymbol{a})$ is the prior, and Z is the evidence. We follow Refs. [5, 45] and discretize the integrals in Eqs. (10) and (11) that lead to the introduction of weights w_k related to the corresponding χ^2's as

$$w_k = \frac{\exp\left[-\frac{1}{2}\,\chi^2(\boldsymbol{a}_k)\right]\pi(\boldsymbol{a}_k)}{\sum_k w_k}\,. \tag{13}$$

The priors $\pi(\boldsymbol{a})$ are obtained using the Monte Carlo (MC) procedure described in the Appendix A of Ref. [2]. Then, we generate N_{set} parameter sets by a multidimensional MC generator, utilizing the covariance matrix from the Minuit [46] fit.

In particular, we start with $N_{set} = 10^5$ parameter sets $\boldsymbol{a}_k$ for the "no SB" fit, so that $k \in [1, N_{set}]$ in Eqs. (10) and (11). We then implement the Soffer bound directly on the priors by keeping those sets with $|N^T_{u_v(d_v)}| < 1$: this results in $N_{set} = 15570$ for the "using SB" fit.

The bands and the central lines in Fig. 1 are computed according to Eqs. (10) and (11). Fig. 1 shows the results of the two types of fits. The extracted transversity functions for u_v and d_v flavours, together with their 2σ uncertainty bands, are plotted at $Q^2 = 4$ GeV^2. The Soffer bound at $Q^2 = 4$ GeV^2 for the two flavours is also shown, with a $\pm 10\%$ variation representing an uncertainty estimate on their central values. The grey areas are the ones outside the existing data, that lies in the range $0.035 \lesssim x \lesssim 0.29$, corresponding to the smallest and highest x value respectively probed by the HERMES and COMPASS Collaborations.

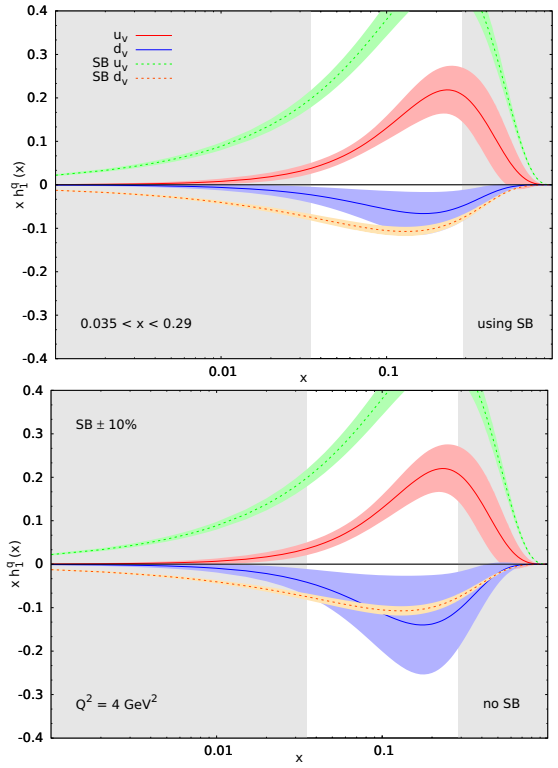

Figure 1: Transversity functions for u_v (red) and d_v (blue) flavours from a global fit to SIDIS and e^+e^- data at $Q^2 = 4$ GeV^2. Upper panel: results with automatic fulfillment of the Soffer Bound ($|N^T_{u_v(d_v)}| \leq 1$). Lower panel: results with no constraint on $N^T_{u_v(d_v)}$. Error bands on the fitted functions are at 2σ. The corresponding Soffer bound, computed with CTEQ66 [40] PDFs and DSSV [39] helicity distributions, is also shown for u_v (green) and d_v (orange), together with a $\pm 10\%$ variation. The white area represents the bulk of the data; outside that region no datapoints are present in the fit.

Besides the differences showed in Fig. 1, we underline that the two extractions have essentially the same statistical significance, rendering similar minimum χ^2's ($\chi^2_{\rm min} = 251.23$ and $\chi^2_{\rm min} = 250.21$ for the "using SB" and "no SB" cases, respectively), and essentially the same $\chi^2_{\rm dof} \simeq 0.93$ for the $N_{\rm par} = 9$ parameter fit.

First of all, we notice that, since the helicity distribution for the d_v quark flavour is negative, the corresponding SB is much more stringent with respect to the u_v one. So, in extracting $h_1^{d_v}(x)$, there is less room for the parameters to vary. We also mention that, in all previous fits, $N^T_{d_v}$ was almost always saturating its lower bound [3, 18].

In the upper panel of Fig. 1, as expected, we observe two extracted functions comparable to the existing extractions in Refs. [3, 18, 23] and respecting the SB for both flavours used in extraction. For the extraction corresponding to "no SB", lower panel of Fig. 1, we can note the following:

(i) when relaxing the constraint on $N_T^{u_v}$, the corresponding transversity function does not essentially change with respect to the one in the upper panel;

(ii) conversely, the d_v transversity function tends to violate its Soffer bound, especially in the region where

data are present;

(iii) while the uncertainty bands of the two extracted $h_1^{u_v}$ are quite similar, there is a significant difference between the uncertainties of $h_1^{d_v}$.

Now, we have to estimate the statistical significance of the violation of the SB for the down-quark transversity function shown in Fig. 1. To this aim, we use a simple z-score method to measure whether we are observing a statistically significant deviation from the zero hypothesis, i.e. the fulfillment of the SB by the d_v transversity function. The z-score is generally defined as

$$z = \frac{x - \mu}{\sigma}\,, \tag{14}$$

and tells us how many standard deviations σ we are far from the mean μ for the point x. In the case of the extracted d_v transversity function, we have $-0.9 \leq z \leq -0.3$ for the whole region, that means that the SB for down quark is well within 1σ deviation and we can conclude that the violation is not statistically significant.

Another aspect is related to the exploration of the parameter space. While the uncertainty on u_v transversity function is essentially unchanged when relaxing the initial constraint, this is not the case for the d_v one.

Furthermore, as mentioned in Ref. [5], the exploration of the parameter space starting from a single fit may lead to incorrect estimates of both mean values and errors of observables and/or extracted parameters. We can demonstrate it explicitly as follows. We perform the constrained "using SB" fit that turns in the saturation of the normalization parameter $N_{d_v}^T = -1$. We point out that, when requesting parameters $N_{u_v(d_v)}^T$ to be limited between -1 and $+1$, the minimizer (Minuit [46]) maps this region onto the unbound region using a arcsin function. Once the fitted parameter is close to the bound value (± 1) this means $\pm\infty$ for the internal parameter of the minimizer. This prevents to explore all regions in the parameter space compatible with the theoretical expectations and with the calculated 2σ error without imposing any bound on parameters. If we now generate the priors using the covariance matrix, the resulting distributions show artificially small errors for the d-quark transversity, see Fig. 2. When the transversity for d quarks saturates, as happens at $x \sim 0.2$, the error becomes extremely small (see green band in Fig. 2). This behavior is typical for constrained fits, see Fig. 4 of Ref [9] or Fig. 8 of Ref. [24]. SIDIS process is dominated by u-quark contribution and thus one expects the relative precision for d quark to be worse with respect to the one reachable for u quark. This is clearly not the case for the d-quark green band in Fig. 2 when compared to the u-quark one in Fig. 1.

Indeed, there exist configurations, compatible with the SB, that are not explored when the constraint on the N_q^T parameters is imposed directly in the fit. This issue was mitigated in Refs. [3, 18] by generating several hundred thousands of parameter sets and in Ref. [11] by using the Lagrange multiplier method instead of imposing direct constraints on the parameters.

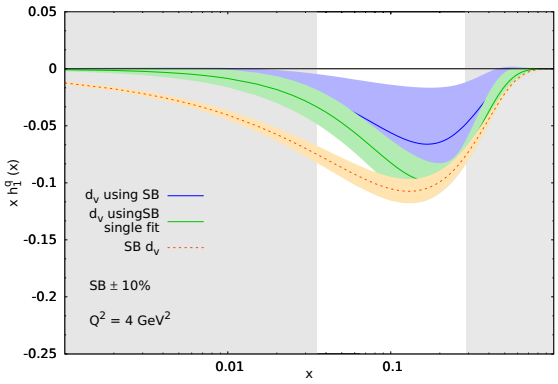

Figure 2: Transversity functions for d_v flavour from a global fit to SIDIS and e^+e^- data at $Q^2 = 4$ GeV^2. Blue band corresponds to usage of priors from Fig. 1, while green band corresponds to priors generated from constrained fit $|N_{d_v}^T| \leq 1$ directly. Error bands on the fitted functions are at 2σ. The corresponding Soffer bound, computed with CTEQ66 [40] PDFs and DSSV [39] helicity distributions, is also shown, together with a $\pm 10\%$ variation. The white area represents the region of the bulk of the data; outside that region no datapoints are present in the fit.

3. Tensor charges

The contribution to the tensor charge of the nucleon from quark q is the first Mellin moment of the non-singlet quark combination

$$\delta q = \int_0^1 \left[h_1^q(x) - h_1^{\bar{q}}(x)\right]\, dx. \tag{15}$$

The isovector combination, g_T, is of particular interest and can be calculated relatively easily on the lattice [47]:

$$g_T = \delta u - \delta d. \tag{16}$$

In our analysis we have $h_1^{\bar{q}} \equiv 0$ and thus we compute valence quark tensor charges as

$$\delta q_v = \int_0^1 h_1^{q_v}(x)\, dx. \tag{17}$$

It is also useful to mention that truncated charges can be built, upon integrating in Eq. (17) between the experimental minimum and maximum x values, $x_{\min}$ and $x_{\max}$ respectively.

As g_T is related to BSM effects [19–22], a phenomenological extraction of the transversity functions can be used in principle to put a limit on the strength of this potential non-standard interactions. At the same time, another means for putting limits on these BSM signals is represented by the lattice QCD estimates of g_T. For a comprehensive review of lattice results, see Ref. [47] and references therein.

Tensions have been observed [25] between phenomenological estimates and lattice QCD calculations of g_T and

individual quark contributions. In fact, δu_v values from phenomenology seem to be incompatible with the lattice ones, and g_T values calculated on the lattice are found to be higher than the ones for most phenomenological analyses [10]. Lattice results are approximately in the range $0.9 \lesssim g_T \lesssim 1.1$, and with very tiny errors, for instance 0.926(32) from a recent study in Ref. [48]. It is then interesting to see the impact of the results presented in Section 2 on the phenomenological estimates of the tensor charges.

By integrating the two couples of extracted transversity functions of Fig. 1, we calculate for every MC set the corresponding tensor charges, δu_v and δd_v, and thus the corresponding isovector tensor charge, g_T. The corresponding central values and errors are again computed according to Eqs. (10) and (11).

To begin with, we can check the effect of relaxing the hypothesis $|N_q^T| \leq 1$ on the tensor charges distributions. Fig. 3 shows the distribution of δu_v (upper panel) and δd_v (lower panel) calculated at $Q^2 = 4\,\mathrm{GeV}^2$, the usual energy scale adopted to compare tensor charges calculated on the basis of phenomenological analyses and lattice QCD estimates. The labels "using SB" and "no SB" have the same meaning as in Fig. 1. As one could expect, while relaxing the initial constraint, the δu_v distribution does not change much, thus reflecting the very small difference observed in the extracted $h_1^{u_v}$ in Fig. 1. At variance with this, the δd_v distribution dramatically changes, reflecting once more what has been observed for the fitted d_v transversity function in Fig. 1.

For the individual quark distributions, we find that both δu_v and δd_v are different from lattice computations, 0.716(28) and $-0.210(11)$ respectively found in Ref. [48], see Table. 1. Although these results do not ease the tension between phenomenological and lattice QCD estimates of δu_v and δd_v; they actually have an effect on the isovector tensor charge estimates.

Fig. 4 shows the distribution of g_T values at $Q^2 = 4\,\mathrm{GeV}^2$ for the "using SB" and "no SB" case. In relaxing the initial constraint on the N_q^T parameters, the g_T distribution broadens. This broadening is due to the changes in the δd_v distribution, and mitigates the existing tension between phenomenological calculation and lattice QCD estimates. Indeed, the peak of the "no SB" g_T distribution moves toward the range of lattice g_T estimates, and its tail overlaps with the lattice QCD range, $0.9 \lesssim g_T \lesssim 1.1$. In this sense, by relaxing the initial request of automatic fulfillment of the Soffer bound, the phenomenological analysis is able to explore portion of the parameter space that are less in tension with g_T estimates on the lattice.

A summary of the results for the tensor charges, δu_v and δd_v, and for the isovector tensor charge, g_T calculated at $Q^2 = 4$ GeV^2, are presented in Table 1. Expectation values and standard deviations are calculated using Eq. (10) and the square root of Eq. (11). The quoted errors are at 2σ.

A word of caution and some comments are in order.

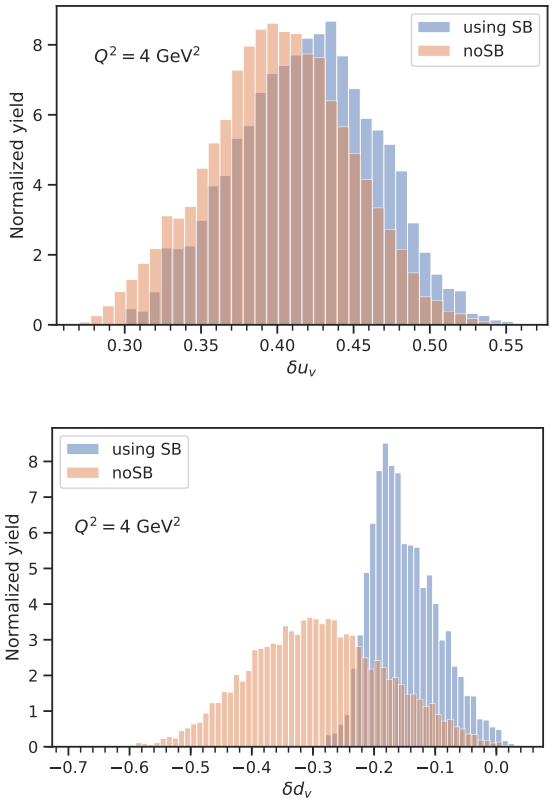

Figure 3: Distributions of the tensor charges for u_v (upper panel) and d_v (lower panel) at $Q^2 = 4\,\mathrm{GeV}^2$. The tensor charges are calculated using the extracted transversity distributions of Fig. 1, integrated over the full range $0 \leq x \leq 1$. Labels "using SB" and "no SB" have the same meaning as in Fig. 1.

There are in fact some aspects to be stressed, that would help in enlighten the current knowledge on transversity and on tensor charges.

As already mentioned, the covered x range in the phenomenological extractions is quite limited, namely $0.035 \lesssim x \lesssim 0.29$. This means that, when calculating δq and g_T, most of the computation is given by an extrapolation based on the adopted model and outside this x range. In this respect, loosening some initial constraints can help in reducing the effect of such extrapolation, but also lead to different results and, in turn, different interpretation. Furthermore, we have to stress that lattice calculations are also based on some specific assumptions such as choice of the action, lattice spacing, etc, and that are performed considering matrix elements over the full x range. Therefore, the comparison between phenomenological and lattice results should be done prudently.

We also notice that, in Ref. [5], a similar analysis has been performed by including lattice data on g_T directly into the fit procedure. The two transversity parametrizations used here and by Lin et al. are quite similar, but the fit of Ref. [5] was performed with different sets of fit parameters and different choices for the collinear PDFs and FFs. Moreover, in order to use SB, we parametrize transversity proportional to SB, while Ref. [5] used a generic x-

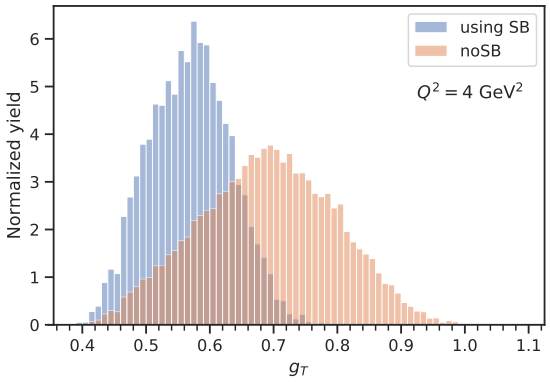

Figure 4: Distributions of the isovector tensor charge, g_T, at $Q^2 = 4\,\mathrm{GeV}^2$. The calculation is performed using the extracted transversity distributions of Fig. 1, integrated over the full range $0 \leq x \leq 1$. Labels "using SB" and "no SB" have the same meaning as in Fig. 1.

	δu_v	δd_v	g_T
	$Q^2 = 4\,\mathrm{GeV}^2$		
using SB	0.42 ± 0.09	-0.15 ± 0.11	0.57 ± 0.13
no SB	0.40 ± 0.09	-0.29 ± 0.22	0.69 ± 0.21

Table 1: Summary of the results at $Q^2 = 4\,\mathrm{GeV}^2$ for the tensor charges and the isovector tensor charge calculations, under the "using SB" and the "no SB" hypotheses. Expectation values and standard deviations are calculated using Eq. (10) and the square root of Eq. (11). The quoted errors are at 2σ.

dependent form. Nonetheless, the results presented in Fig. 3 of Ref. [5] is compatible with our results. Notice that Ref. [5] performed only analysis of SIDIS data, whereas we use both SIDIS and e^+e^- data.

It would be certainly interesting to extend such a kind of study to similar analyses performed in the collinear framework, such as the one by Bacchetta and Radici [10], where independent datasets are used and where, within a different parametrization for transversity, the automatic fulfillment of the Soffer bound is also achieved. In fact, the recent study of Ref. [11] does study the influence of SB on the extraction of transversity. The results of the current study are in agreement, within the errors, with those of Refs. [10, 11]. Notice that the contribution of down quark varies the most between different studies, ours and Refs. [2, 5, 10, 11]. This is not unexpected: down quark functions are less constrained by the experimental data, the bound is more stringent, and thus one is to expect the larger variation of results based on methodology of the fit and used parametrization.

4. Conclusions

In this letter we have studied the role of initial assumptions in phenomenological analyses for transversity function from SIDIS data. The tranversity distributions are usually parametrized in terms of their corresponding Soffer bounds and, upon some choices, the bound is automatically fulfilled throughout the analysis.

By means of an explicit example, we have shown that, by relaxing the initial assumptions on the parameters that ensure the automatic fulfilment of the bound, we could obtain interesting information on the size of the violation of the Soffer bound observed in current SIDIS data. It turns out that there is no statistically significant violation of such bound. Moreover, loosening the initial choices on the parameters has allowed us to explore better the parameter space and have more reliable estimates on the errors, in particular for down quark transversity.

Using then the extracted transversity functions, we have calculated the tensor charges for u_v and d_v quark flavours and, consequently, the isovector tensor charge, g_T. Another effect of loosening the initial constraints on the parameters for transversity is on the tensor charges estimates. In fact, the existing tensions observed between phenomenological and lattice QCD estimates of g_T are eased, and the g_T values distribution moves towards the range of lattice QCD estimates. Nonetheless, the discrepancy observed for δu_v persists.

Current SIDIS data are, at the moment, not sufficient to constrain the valence transversity functions and, in turn, the tensor charges. The probed x range, ($0.035 \lesssim x \lesssim 0.29$), is still too narrow to avoid the effects of extrapolations made in the integration needed to compute tensor charges and g_T. If we calculate truncated values for "no SB" fit of δu_v, δd_v, and g_T, we obtain 0.29 ± 0.03, -0.23 ± 0.10, and 0.52 ± 0.10 respectively (to be compared with the values in Table 1). Thus, around 30% of the tensor charge value results from an extrapolation to an unexplored region of x.

In this respect, new SIDIS data from the future Electron Ion Collider and Jefferson Lab could definitely help in reducing the effect from this model dependence and expand the region of explored values of x. Another avenue of constraining transversity is the addition of the data from other processes, where transversity is probed into a global fit, such as the left-right asymmetry measured in polarised proton-proton scattering.

In conclusion, similar educated analyses in different frameworks would certainly be helpful in pinning down the transversity function and, in turn, constraining the tensor charges and the isovector one more reliably.

Acknowledgments

This paper was supported in part by the National Science Foundation under Grant No. PHY-1623454 (A.P., C.F.), the DOE Contract No. DE-AC05-06OR23177 (A.P.), under which Jefferson Science Associates, LLC operates Jefferson Lab, by the European Union's Horizon 2020 research and innovation programme under grant agreement No. 824093 (C.F.), and by Regione Autonoma della Sardegna (C.F.). C.F. is thankful to Penn State Berks for

hospitality and support for his visit during which part of the project was done.

References

[1] J. P. Ralston, D. E. Soper, Production of Dimuons from High-Energy Polarized Proton Proton Collisions, Nucl. Phys. B152 (1979) 109 (1979). doi:10.1016/0550-3213(79)90082-8.

[2] M. Anselmino, M. Boglione, U. D'Alesio, A. Kotzinian, S. Melis, F. Murgia, A. Prokudin, C. Turk, Sivers effect for pion and kaon production in Semi-Inclusive Deep Inelastic Scattering, Eur. Phys. J. A39 (2009) 89–100 (2009). arXiv:0805.2677, doi:10.1140/epja/i2008-10697-y.

[3] M. Anselmino, M. Boglione, U. D'Alesio, S. Melis, F. Murgia, A. Prokudin, Simultaneous extraction of transversity and Collins functions from new SIDIS and e^+e^- data, Phys. Rev. D87 (2013) 094019 (2013). arXiv:1303.3822, doi:10.1103/PhysRevD.87.094019.

[4] Z.-B. Kang, A. Prokudin, P. Sun, F. Yuan, Extraction of Quark Transversity Distribution and Collins Fragmentation Functions with QCD Evolution, Phys. Rev. D93 (1) (2016) 014009 (2016). arXiv:1505.05589, doi:10.1103/PhysRevD.93.014009.

[5] H.-W. Lin, W. Melnitchouk, A. Prokudin, N. Sato, H. Shows, First Monte Carlo Global Analysis of Nucleon Transversity with Lattice QCD Constraints, Phys. Rev. Lett. 120 (15) (2018) 152502 (2018). arXiv:1710.09858, doi:10.1103/PhysRevLett.120.152502.

[6] J. C. Collins, Fragmentation of transversely polarized quarks probed in transverse momentum distributions, Nucl. Phys. B396 (1993) 161–182 (1993). arXiv:hep-ph/9208213, doi:10.1016/0550-3213(93)90262-N.

[7] R. L. Jaffe, X.-m. Jin, J. Tang, Interference fragmentation functions and the nucleon's transversity, Phys. Rev. Lett. 80 (1998) 1166–1169 (1998). arXiv:hep-ph/9709322, doi:10.1103/PhysRevLett.80.1166.

[8] M. Radici, R. Jakob, A. Bianconi, Accessing transversity with interference fragmentation functions, Phys. Rev. D65 (2002) 074031 (2002). arXiv:hep-ph/0110252, doi:10.1103/PhysRevD.65.074031.

[9] A. Bacchetta, A. Courtoy, M. Radici, First extraction of valence transversities in a collinear framework, JHEP 03 (2013) 119 (2013). arXiv:1212.3568, doi:10.1007/JHEP03(2013)119.

[10] M. Radici, A. Bacchetta, First extraction of transversity from a global analysis of electron-proton and proton-proton data, Phys. Rev. Lett. 120 (19) (2018) 192001 (2018). arXiv:1802.05212, doi:10.1103/PhysRevLett.120.192001.

[11] J. Benel, A. Courtoy, R. Ferro-Hernandez, Constrained fit of the valence transversity distributions from dihadron production (2019). arXiv:1912.03289.

[12] R. L. Jaffe, X.-D. Ji, Chiral odd parton distributions and polarized Drell-Yan, Phys. Rev. Lett. 67 (1991) 552–555 (1991). doi:10.1103/PhysRevLett.67.552.

[13] X. Artru, M. Mekhfi, Transversely Polarized Parton Densities, their Evolution and their Measurement, Z. Phys. C45 (1990) 669 (1990). doi:10.1007/BF01556280.

[14] J. Soffer, Positivity constraints for spin dependent parton distributions, Phys. Rev. Lett. 74 (1995) 1292–1294 (1995). arXiv:hep-ph/9409254, doi:10.1103/PhysRevLett.74.1292.

[15] V. Barone, On the QCD evolution of the transversity distribution, Phys. Lett. B409 (1997) 499–502 (1997). arXiv:hep-ph/9703343, doi:10.1016/S0370-2693(97)00875-7.

[16] W. Vogelsang, Next-to-leading order evolution of transversity distributions and Soffer's inequality, Phys. Rev. D57 (1998) 1886–1894 (1998). arXiv:hep-ph/9706511, doi:10.1103/PhysRevD.57.1886.

[17] J. P. Ralston, Exploring Confinement with Spin, in: Transversity 2008: 2nd International Workshop on Transverse Polarization Phenomena in Hard Processes Ferrara, Italy, May 28-31, 2008, 2008 (2008). arXiv:0810.0871, doi:10.1142/9789814277785_0028.

[18] M. Anselmino, M. Boglione, U. D'Alesio, J. O. Gonzalez Hernandez, S. Melis, F. Murgia, A. Prokudin, Collins functions for pions from SIDIS and new e^+e^- data: a first glance at their transverse momentum dependence, Phys. Rev. D92 (11) (2015) 114023 (2015). arXiv:1510.05389, doi:10.1103/PhysRevD.92.114023.

[19] V. Cirigliano, J. Jenkins, M. Gonzalez-Alonso, Semileptonic decays of light quarks beyond the Standard Model, Nucl. Phys. B830 (2010) 95–115 (2010). arXiv:0908.1754, doi:10.1016/j.nuclphysb.2009.12.020.

[20] T. Bhattacharya, V. Cirigliano, S. D. Cohen, A. Filipuzzi, M. Gonzalez-Alonso, M. L. Graesser, R. Gupta, H.-W. Lin, Probing novel scalar and tensor interactions from (ultra)cold neutrons to the LHC, Phys. Rev. D85 (2012) 054512 (2012). arXiv:1110.6448, doi:10.1103/PhysRevD.85.054512.

[21] A. Courtoy, S. Baeßler, M. González-Alonso, S. Liuti, Beyond-Standard-Model tensor interaction and hadron phenomenology, Phys. Rev. Lett. 115 (2015) 162001 (2015). arXiv:1503.06814, doi:10.1103/PhysRevLett.115.162001.

[22] N. Yamanaka, B. K. Sahoo, N. Yoshinaga, T. Sato, K. Asahi, B. P. Das, Probing exotic phenomena at the interface of nuclear and particle physics with the electric dipole moments of diamagnetic atoms: A unique window to hadronic and semi-leptonic CP violation, Eur. Phys. J. A53 (3) (2017) 54 (2017). arXiv:1703.01570, doi:10.1140/epja/i2017-12237-2.

[23] M. Anselmino, M. Boglione, U. D'Alesio, A. Kotzinian, F. Murgia, A. Prokudin, C. Turk, Transversity and Collins functions from SIDIS and e^+e^- data, Phys. Rev. D75 (2007) 054032 (2007). arXiv:hep-ph/0701006, doi:10.1103/PhysRevD.75.054032.

[24] M. Radici, A. Courtoy, A. Bacchetta, M. Guagnelli, Improved extraction of valence transversity distributions from inclusive dihadron production, JHEP 05 (2015) 123 (2015). arXiv:1503.03495, doi:10.1007/JHEP05(2015)123.

[25] M. Radici, Update on phenomenological extraction of the proton tensor charge, PoS DIS2019 (2019) 199 (2019). doi:10.22323/1.352.0199.

[26] A. Airapetian, et al., Observation of the Naive-T-odd Sivers Effect in Deep-Inelastic Scattering, Phys. Rev. Lett. 103 (2009) 152002 (2009). arXiv:0906.3918, doi:10.1103/PhysRevLett.103.152002.

[27] M. Alekseev, et al., Collins and Sivers asymmetries for pions and kaons in muon-deuteron DIS, Phys. Lett. B673 (2009) 127–135 (2009). arXiv:0802.2160, doi:10.1016/j.physletb.2009.01.060.

[28] C. Adolph, et al., Collins and Sivers asymmetries in muonproduction of pions and kaons off transversely polarised protons, Phys. Lett. B744 (2015) 250–259 (2015). arXiv:1408.4405, doi:10.1016/j.physletb.2015.03.056.

[29] X. Qian, et al., Single Spin Asymmetries in Charged Pion Production from Semi-Inclusive Deep Inelastic Scattering on a Transversely Polarized ^{3}He Target, Phys. Rev. Lett. 107 (2011) 072003 (2011). arXiv:1106.0363, doi:10.1103/PhysRevLett.107.072003.

[30] A. Kotzinian, New quark distributions and semiinclusive electroproduction on the polarized nucleons, Nucl. Phys. B441 (1995) 234–248 (1995). arXiv:hep-ph/9412283, doi:10.1016/0550-3213(95)00098-D.

[31] P. J. Mulders, R. D. Tangerman, The Complete tree level result up to order 1/Q for polarized deep inelastic leptoproduction, Nucl. Phys. B461 (1996) 197–237, [Erratum: Nucl. Phys.B484,538(1997)] (1996). arXiv:hep-ph/9510301, doi:10.1016/S0550-3213(96)00648-7,10.1016/0550-3213(95)00632-X.

[32] A. Bacchetta, M. Diehl, K. Goeke, A. Metz, P. J. Mulders, M. Schlegel, Semi-inclusive deep inelastic scattering at small transverse momentum, JHEP 02 (2007) 093 (2007). arXiv:hep-ph/0611265, doi:10.1088/1126-6708/2007/02/093.

[33] D. Boer, R. Jakob, P. J. Mulders, Asymmetries in polarized hadron production in e+ e- annihilation up to order 1/Q, Nucl. Phys. B504 (1997) 345–380 (1997). arXiv:hep-ph/9702281,

doi:10.1016/S0550-3213(97)00456-2.

[34] R. Seidl, et al., Measurement of azimuthal asymmetries in inclusive production of hadron pairs in e^+e^- annihilation at $\sqrt{s} = 10.58$ GeV, Phys. Rev. D78 (2008) 032011, [Erratum: Phys. Rev.D86,039905(2012)] (2008). arXiv:0805.2975, doi:10.1103/PhysRevD.78.032011,10.1103/PhysRevD.86.039905.

[35] J. P. Lees, et al., Measurement of Collins asymmetries in inclusive production of charged pion pairs in e^+e^- annihilation at BABAR, Phys. Rev. D90 (5) (2014) 052003 (2014). arXiv:1309.5278, doi:10.1103/PhysRevD.90.052003.

[36] M. Ablikim, et al., Measurement of azimuthal asymmetries in inclusive charged dipion production in e^+e^- annihilations at $\sqrt{s} = 3.65$ GeV, Phys. Rev. Lett. 116 (4) (2016) 042001 (2016). arXiv:1507.06824, doi:10.1103/PhysRevLett.116.042001.

[37] A. Airapetian, et al., Effects of transversity in deep-inelastic scattering by polarized protons, Phys. Lett. B693 (2010) 11–16 (2010). arXiv:1006.4221, doi:10.1016/j.physletb.2010.08.012.

[38] M. Anselmino, M. Boglione, J. O. Gonzalez Hernandez, S. Melis, A. Prokudin, Unpolarised Transverse Momentum Dependent Distribution and Fragmentation Functions from SIDIS Multiplicities, JHEP 04 (2014) 005 (2014). arXiv:1312.6261, doi:10.1007/JHEP04(2014)005.

[39] D. de Florian, R. Sassot, M. Stratmann, W. Vogelsang, Extraction of spin-dependent parton densities and their uncertainties, Phys. Rev. D80 (2009) 034030 (2009). arXiv:0904.3821, doi:10.1103/PhysRevD.80.034030.

[40] P. M. Nadolsky, H.-L. Lai, Q.-H. Cao, J. Huston, J. Pumplin, D. Stump, W.-K. Tung, C.-P. Yuan, Implications of CTEQ global analysis for collider observables, Phys. Rev. D78 (2008) 013004 (2008). arXiv:0802.0007, doi:10.1103/PhysRevD.78.013004.

[41] D. de Florian, R. Sassot, M. Epele, R. J. Hernández-Pinto, M. Stratmann, Parton-to-Pion Fragmentation Reloaded, Phys. Rev. D91 (1) (2015) 014035 (2015). arXiv:1410.6027, doi:10.1103/PhysRevD.91.014035.

[42] A. Courtoy, A. Bacchetta, M. Radici, A. Bianconi, First extraction of Interference Fragmentation Functions from e^+e^- data, Phys. Rev. D85 (2012) 114023 (2012). arXiv:1202.0323, doi:10.1103/PhysRevD.85.114023.

[43] A. Bacchetta, private communication (2015).

[44] G. P. Salam, J. Rojo, A Higher Order Perturbative Parton Evolution Toolkit (HOPPET), Comput. Phys. Commun. 180 (2009) 120–156 (2009). arXiv:0804.3755, doi:10.1016/j.cpc.2008.08.010.

[45] N. Sato, J. J. Ethier, W. Melnitchouk, M. Hirai, S. Kumano, A. Accardi, First Monte Carlo analysis of fragmentation functions from single-inclusive e^+e^- annihilation, Phys. Rev. D94 (11) (2016) 114004 (2016). arXiv:1609.00899, doi:10.1103/PhysRevD.94.114004.

[46] F. James, M. Roos, Minuit: A System for Function Minimization and Analysis of the Parameter Errors and Correlations, Comput. Phys. Commun. 10 (1975) 343–367 (1975). doi:10.1016/0010-4655(75)90039-9.

[47] C. Alexandrou, Novel applications of Lattice QCD: Parton Distributions, proton charge radius and neutron electric dipole moment, EPJ Web Conf. 137 (2017) 01004 (2017). arXiv:1612.04644, doi:10.1051/epjconf/201713701004.

[48] C. Alexandrou, S. Bacchio, M. Constantinou, J. Finkenrath, K. Hadjiyiannakou, K. Jansen, G. Koutsou, A. Vaquero Aviles-Casco, The nucleon axial, tensor and scalar charges and σ-terms in lattice QCD (2019). arXiv:1909.00485.